

# DIRECT NUMERICAL SIMULATION AND THEORY OF A WALL-BOUNDED FLOW WITH ZERO SKIN FRICTION

*G.N. Coleman<sup>1</sup>, S. Pirozzoli<sup>2</sup>, M. Quadrio<sup>3</sup> and P.R. Spalart<sup>4</sup>*

<sup>1</sup> *NASA Langley Research Center, Hampton, VA 23681, USA*

<sup>2</sup> *Sapienza Università di Roma, Via Eudossiana 18, 00184 Roma, Italy*

<sup>3</sup> *Politecnico di Milano, Via La Masa 34, 20156 Milano, Italy*

<sup>4</sup> *Boeing Commercial Airplanes, P.O. Box 3707, Seattle, WA 98124, USA*

[g.n.coleman@nasa.gov](mailto:g.n.coleman@nasa.gov)

## Abstract

We study turbulent plane Couette-Poiseuille (CP) flows in which the conditions (relative wall velocity  $\Delta U_w \equiv 2U_w$  and pressure gradient  $dP/dx$ ) are adjusted to produce zero mean skin friction on one of the walls, denoted by APG for adverse pressure gradient. The other wall, FPG for favorable pressure gradient, provides the friction velocity  $u_\tau$ , and  $h$  is the half-height of the channel. This leads to a one-dimensional family of flows of varying Reynolds number  $Re \equiv U_w h/\nu$ . We apply three codes, and cover three Reynolds numbers stepping by a factor of 2 each time. The agreement between codes is very good. The theoretical questions involve Reynolds-number independence in both the core region (free of local viscous effects) and the two wall regions. The core region follows Townsend's hypothesis of universal behavior for the velocity and shear stress, when they are normalized with  $u_\tau$  and  $h$ ; universality is not observed for all the Reynolds stresses. The FPG wall region obeys the classical law of the wall, again for velocity and shear stress, but suggesting a low value for the Karman constant  $\kappa$ , between 0.36 and 0.37. For the APG wall region, Stratford conjectured universal behavior when normalized with the pressure gradient, leading to a square-root law for the velocity. The literature, also covering other flows, is ambiguous. Our results are very consistent with both of Stratford's conjectures, suggesting that at least in this idealized flow geometry the theory is successful like it was for the classical law of the wall, and we know the constants of the law within a 10% bracket. On the other hand, again that does not extend to all the Reynolds stresses.

## 1 Introduction

The ultimate aim of this study is to test two theoretical conjectures applied to the zero-skin-friction CP flow, which we will name CP0. The first conjecture is that the velocity profile near the frictionless wall is universal (independent of the flow Reynolds number

Re) when velocity and wall distance are both normalized by the pressure gradient and the kinematic viscosity  $\nu$ , so that

$$U^- = \mathcal{F}(y^-), \quad (1)$$

where  $U^- \equiv U/u_p$ ,  $y^- \equiv y_w u_p/\nu$ ,  $y_w$  is the wall-normal distance from the frictionless wall,  $u_p^3 \equiv \nu d(P/\rho)/dx$  and  $\rho$  is the (constant) fluid density. The second conjecture is that for large  $y^-$ , allowed by high enough Re, the velocity profile will include a square-root layer, with (1) taking the form

$$U^- = B\sqrt{y^-} + C, \quad (2)$$

where  $B$  and  $C$  are nondimensional universal constants. These conjectures, which we shall refer to respectively as (I) and (II), come from reasoning, first proposed by Stratford (1959), equivalent to those that produce the classical Law of the Wall and logarithmic layer; the skin friction being zero, the normalization is built on the pressure gradient instead.

Although CP0 flow arguably provides the best chance of success for conjectures (I) and (II), its study to date has yet to provide clear conclusions. Schlichting & Gersten (2000) cite experiments (not in the CP0 flow) for which the 'universal constants' range as widely as  $2.5 < B < 4.9$  and  $-3.2 < C < 2.2$ , while our direct numerical simulation (DNS) of CP0 flow (Coleman & Spalart 2015; hereinafter CS15) revealed significant differences with the earlier DNS of Pirozzoli, Bernardini & Orlandi (2011) (henceforth PBO11); although both appear to support the  $\sqrt{y^-}$  behavior, PBO11 yields  $(B, C) = (3.6, -2.65)$  while CS15 suggests  $(2.2, -2.05)$ . The primary objective of this paper is to resolve this discrepancy, via a series of new DNS, and thereby provide unambiguous evidence either for or against conjectures (I) and (II).

In addition to being a testbed for the zero-skin-friction scaling, this flow also satisfies the conditions assumed by Townsend (1976) in his derivation of Reynolds-number similarity for the mean velocity profile  $U(y)$  in the core of a parallel wall-bounded turbulent shear flow (see his §5.3), which in the present

Case	Re	Code	$\frac{d(P/\rho U_w^2)}{d(x/h)}$	$\tau_{w,APG}/\rho u_\tau^2$	$N_x$	$\Delta x^+$	$N_y$	$y_{10}^+$	$N_z$	$\Delta z^+$	$T_A U_w/h$	$\xi$
A3000	3000	A	-0.0044	$+1.5 \times 10^{-4}$	512	6.9	192	2.4	384	4.6	2000	0.03
B3000	3000	B	-0.0044	$+2 \times 10^{-3}$	512	6.9	151	10.4	512	3.5	2000	0.08
C3000	3000	C	-0.0044	$-6 \times 10^{-4}$	576	6.2	257	1.7	432	4.1	789	0.05
A6000	6000	A	Variable <sup>†</sup>	0	1024	6.4	384	1.8	768	4.3	2000	0.02
C6000a	6000	C	-0.0037836	$-2 \times 10^{-3}$	1152	5.7	385	1.4	864	3.8	1900	0.18
C6000b	6000	C	-0.0037836	$-7 \times 10^{-4}$	576	11.4	257	3.2	864	3.8	2240	0.08
C12000	12 000	C	-0.0032894	$+6 \times 10^{-4}$	1152	10.7	385	2.7	1536	4.0	751	0.65

Table 1: CP0 case parameters. Details of DNS algorithms given in Pirozzoli *et al.* (2011) (Code A; see also Orlandi 2000), Luchini & Quadrio (2006) (Code B) and Johnstone *et al.* (2010) (Code C). Streamwise  $\Lambda_x$  and spanwise  $\Lambda_z$  domain sizes are the same for all cases, with  $\Lambda_x/h = 4\pi$  and  $\Lambda_z/h = 2\pi$ . <sup>†</sup>Case A6000 uses a spatially uniform time-dependent pressure gradient adjusted such that the APG-wall shear  $\tau_{w,APG}$  remains identically zero; Cases C6000a, C6000b and C12000 use a fixed pressure gradient of magnitude equal to the average of the time-dependent  $dP/dx$  from Case A6000. Resolution given in terms of equivalent streamwise  $N_x$ , wall-normal  $N_y$  and spanwise  $N_z$  grid points (with de-aliasing in  $x$  and  $z$  for Codes B and C, such that the number of expansion coefficients is 2/3 the number of grid points in these directions), and the resulting FPG-wall units  $\Delta x^+ = \Delta x u_\tau/\nu$ ,  $y_{10}^+ = (h + y_{10}) u_\tau/\nu$  and  $\Delta z^+ = \Delta z u_\tau/\nu$ , where  $\Delta x = \Lambda_x/N_x$ ,  $\Delta z = \Lambda_z/N_z$  and  $y_{10}$  is the  $y$ -coordinate of the 10th grid point from the bottom of the domain. The momentum-imbalance parameter  $\xi$  (which would equal zero for perfect balance) is defined in the text.

context implies

$$\frac{U(y) - U_c}{u_\tau} = \mathcal{F}\left(\frac{y}{h}\right), \quad (3)$$

where  $\tau_w \equiv \rho u_\tau^2$  is the nonzero wall-shear stress (i.e., on the FPG wall, at  $y = -h$ ; cf. Fig. 1) and  $U_c$  is the mean velocity at the channel center,  $y = 0$ . In other words,  $u_\tau$  is the only velocity scale and  $h$  the only length scale for this problem (scaling with  $u_\tau$  and  $h$  or with  $d(P/\rho)/dx$  and  $h$  is actually equivalent), and away from the walls  $\mathcal{F}(y/h)$  is independent of Reynolds number. The degree to which the present results satisfy (3) will also be of great interest, and the FPG wall is of course a candidate for universal behavior, of the common type, extending into the core region.

## 2 Approach and Problem Definition

Results for  $Re = 3000, 6000$  and  $12\,000$  are considered below. The parameters used for the various cases are tabulated in Table 1.

To put this study on as firm a foundation as possible, we apply three separate DNS codes – one finite-difference (Code A; PBO11), one mixed-discretization (Code B; Luchini & Quadrio 2006) and one fully spectral (Code C; Johnstone *et al.* 2010) – to the same flow conditions, with  $Re = 3000$  and  $d(P/\rho)/dx = -0.0044U_w^2/h$ , in the same domain, assuming periodic conditions in the streamwise  $x$  and spanwise  $z$  directions, with periods  $\Lambda_x = 4\pi h$  and  $\Lambda_z = 2\pi h$ . These are respectively denoted Case A3000, B3000 and C3000. This pressure-gradient/wall-velocity combination yields negligible skin friction on the APG wall (Fig. 1), in that the stress on that wall is at most of the order of 0.1% of the FPG-wall value (Table 1). The number of grid points used for each case, and the corresponding spatial resolution in FPG-side wall units, are listed in Table 1.

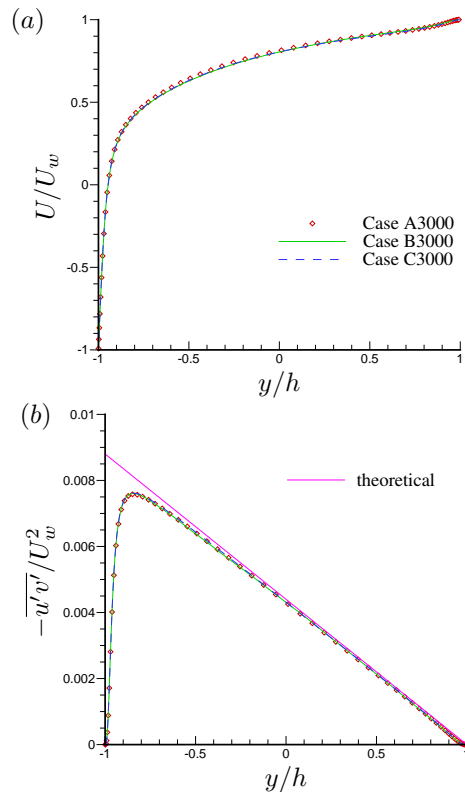


Figure 1: Profiles of (a) mean velocity and (b) Reynolds shear stress for  $Re = 3000$  from three DNS codes. Straight line in (b) indicates total-stress profile defined by pressure gradient.

In most cases, the resolution is within the bounds needed for a spectral discretization (such as that used by Codes B and C) to produce accurate first- and second-order statistics (provided they have been averaged over a sufficient sample) in a turbulent boundary layer with finite skin friction (e.g., (see Table 1 legend),  $\Delta x^+ \leq 12$ ,  $\Delta z^+ \leq 4$ ,  $y_{10}^+ \leq 6$ ; cf. Spalart *et al.* 2009). More direct confirmation of the appropriateness of the resolution, especially on the APG side, will be inferred by comparing results from the different codes. Codes A and C are also applied at  $Re = 6000$ , for Cases A6000, C6000a and C6000b, also with pressure gradients tuned to yield  $dU/dy \approx 0$  (or in the former case,  $dU/dy \equiv 0$ ) on the APG wall; the latter two spectral-code runs are identical except for the streamwise and wall-normal resolution, to demonstrate by their agreement the validity of the resolution used for Case C12000 (cf. Table 1). All runs considered here are in a  $\Lambda_x = 4\pi h$ ,  $\Lambda_z = 2\pi h$  domain. The adequacy of this domain size will be addressed in a future study.

Turbulent initial conditions were obtained either by applying random velocity disturbances across the domain, or from a mature field from another case at lower Reynolds number. In particular, for Case C12000, a Case C6000a field was projected onto a finer grid (Table 1) and the wall velocities adjusted to minimize the changes to net streamwise momentum. This involved invoking (3) in the core region while maintaining the same  $d(P/\rho)/dx$ , and thereby the same  $u_\tau$ , employed for Case C6000a.

The mean-momentum imbalance, and thus a measure of the quality of the statistics, for the various cases is quantified in terms of an integral of the difference squared between the two right-hand-side terms of the streamwise RANS equation. This quantity is defined as

$$\xi = \left[ \frac{1}{2h} \int_{-h}^{+h} \left[ \frac{d\tau}{dy} - \frac{d(P/\rho)}{dx} \right]^2 dy \right]^{\frac{1}{2}} / \frac{-d(P/\rho)}{dx},$$

where  $\tau = \nu dU/dy - \overline{u'v'}$ ; it is included in Table 1.

### 3 Results

The  $Re = 3000$  results from the three codes are presented in Fig. 1. The close agreement points to the accuracy and reliability of the DNS data, at least for this domain size, and to the adequacy of the spatial resolution used in each case (which implies that that used for A3000 and C3000, especially in the wall-normal direction, is much finer than is required to capture faithfully the  $U$  and  $-\overline{u'v'}$  profiles). The APG-side skin friction is also a very discriminating measure of the agreement between codes.

A comparison across all three  $Re$  values is shown in Fig. 2a, in terms of the outer-layer scaling (3), with respect to the friction velocity  $u_\tau$ ; the striking collapse across the core of the flow supports Townsend's assumption that  $u_\tau$  is the relevant outer-layer velocity

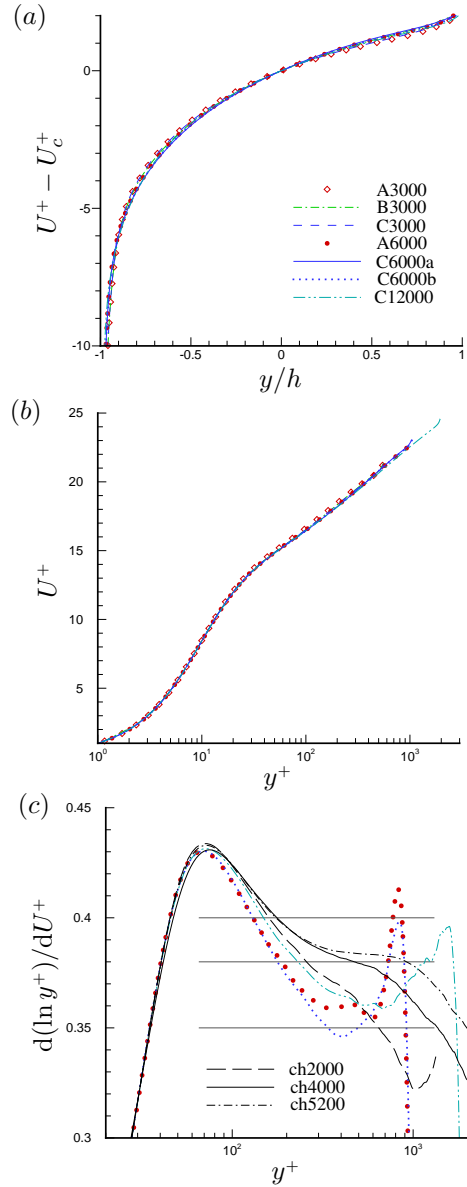


Figure 2: Mean-velocity profiles scaled with respect to  $u_\tau$ , in terms of (a) outer  $y/h$  coordinate (relative to centerline velocity  $U_c^+ = U(0)/u_\tau$ ), (b) inner  $y^+$  coordinate, where  $y^+ = (y+h)u_\tau/\nu$  and (c) Karman measure  $K_m = d(\ln y^+)/dU^+$ . Horizontal lines in (c) indicate  $K_m = 0.35, 0.38$  and  $0.40$ . For  $Re = 3000, 6000$  and  $12000$ , respectively,  $u_\tau/U_w = 0.0938, 0.0867$  and  $0.0813$  such that  $h^+ = 282, 520$  and  $975$  (note that to obtain the same equivalent shear-layer thickness in a plane-channel flow the Reynolds number, based on half-channel-height and friction velocity, would need to be roughly twice these values). Cases ch2000, ch4000 and ch5200 in (c) are from plane-channel ( $U_w \equiv 0$ ) DNS of, respectively, Hoyas & Jiménez (2006) ( $R_\tau = u_\tau h/\nu = 2003$ ), Bernardini *et al.* (2014) ( $R_\tau = 4079$ ) and Lee & Moser (2015) ( $R_\tau = 5186$ ).

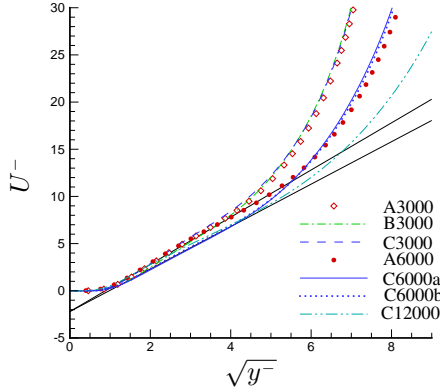


Figure 3: Mean-velocity profiles scaled with respect to  $u_p$  (APG wall), as a function of the nondimensional wall-normal distance  $y^- = (h - y)u_p/\nu$ . For  $\text{Re} = 3000, 6000$  and  $12000$ , respectively,  $u_p/U_w = 0.0114, 0.00858$  and  $0.00650$ , such that  $h^- = 34.1$  and  $51.5$  and  $78.0$ . Straight lines correspond to (2) with  $B = 2.25$  and  $2.50$ , both with  $C = -2.2$ .

scale, and that Reynolds-number effects are limited to thin regions near both walls. (The close agreement between the Case C6000a and C6000b results in this figure, as well as in Fig. 3, indirectly affirms the resolution used for the latter, and thus for Case C12000; cf. Table 1.) The inner scaling for the FPG wall is shown in Fig. 2b for the mean velocity and in Fig. 4a for the Reynolds stresses. The behavior is highly reminiscent of that seen in pure plane-Poiseuille flow. We note the approach towards zero of the pressure gradient with Reynolds number, implied by the reduction in slope of the shear stress profile in Fig. 4a (i.e., that the pressure gradient in wall units  $p^+$  goes to zero as  $\text{Re}$  increases). The logarithmic  $U^+$  profile in Fig. 2b reveals the manner in which this flow essentially doubles the thickness of the inertial sublayer contained between the walls, compared to the plane-channel counterpart.

Fig. 2c presents the ‘Karman Measure’  $K_m \equiv d(\ln y^+)/dU^+$ ; it would be equal to the Karman constant  $\kappa$  in regions that exactly satisfy the logarithmic relationship. That there is no exact plateau, nor even very close agreement past  $y^+ \approx 150$ , even in the higher-Reynolds-number plane channel DNS results of Hoyas & Jiménez (2006), Bernardini, Pirozzoli & Orlandi (2014) and Lee & Moser (2015) also shown in Fig. 2c, is a symptom of the residual uncertainty regarding the log law – its validity, universality, or perhaps more accurately the minimum Reynolds number above which it can be expected. The  $U_w = 0$  channel results appear to be universal up to  $y/h \approx 0.06$ . Even after vast increases in Reynolds number since the 1980s, the DNS findings regarding the log law remain disappointing (actually, the experimental situation is not much better, because recent, careful, high-Reynolds-number experiments disagree substantially over the value of  $\kappa$ ). Note that this presentation mag-

nifies differences, say compared with Fig. 2b, which contains the same information, but this magnification is unavoidable when attempting to determine the second digit of  $\kappa$ . We provisionally interpret Fig. 2c as indicating  $\kappa$  takes a value between 0.36 and 0.37 in our simulations. In the authors’ opinions, this is somewhat outside the accepted range, and therefore more study is needed.

A test of conjectures (I) and (II) (i.e., of Eqs. (1) and (2)) is provided by the  $u_p, \nu$  scaling shown in Fig. 3, which contains the  $\text{Re} = 3000$  profiles from Fig. 1, as well as the results from the  $\text{Re} = 6000$  and  $12000$  runs. Although differences of the order of 1  $U^-$  unit remain, we consider this set of results to be strongly in favor of both conjectures, which is quite a positive outcome. Manual fits suggest the approximate range  $[2.25, 2.50]$  for  $B$  and  $C \approx -2.2$  (see interpolants in Fig. 3). These are considerably tighter than the ranges in place before the present study, even limited to CP0 DNS.

A theoretical concern is that the square-root argument depends on large values of  $y^-$ , just like the logarithmic law appears only for  $y^+ \gg 1$  (in practice, at least 50), and at first sight the  $y^-$  range may not yet be large enough. In other words, the appearance of a square-root layer could appear premature. A counter-argument is the observation that the ratio of the total-to-viscous shear stress within the  $y_w^{1/2}$  regime (where Eq. (2) is valid) is given by  $2(y^-)^{3/2}/B$ ; assuming  $B = \mathcal{O}(2)$  (cf. PBO11; SC15), this implies that even at the bottom of the range of  $U \sim y_w^{1/2}$  behavior shown in Fig. 2a, near  $y^- = 4$ , the turbulent stress is already an order of magnitude larger than the viscous component, and at the upper limit of the validity of (2) found for  $\text{Re} = 6000$ ,  $y^- \approx 20$ , the turbulent-viscous stress ratio is approaching 100. Based on this reasoning ( $(y^-)^{3/2}$ , rather than  $y^-$  or  $(y^-)^{1/2}$ , is the quantity that needs to be ‘large’ for the  $U \sim y_w^{1/2}$  scaling to be valid. The equivalent ratio in a log law is  $\kappa y^+$ , which is only about 40 at  $y^+ = 100$ , where the log law may be reasonably expected to begin. We note that  $(h^-)^{3/2} = (hu_p/\nu)^{3/2} \approx 200$  for the  $\text{Re} = 3000$  flow, and increases to  $\approx 370$  at  $\text{Re} = 6000$  and  $\approx 690$  at  $\text{Re} = 12000$ . (Compare the corresponding increase in the channel half-height in viscous units from  $h^+ = hu_\tau/\nu$  of about 280 to 520 to 975.) These considerations support the relevance of the present DNS as a means to address the validity of (1) and (2), in the sense that the Reynolds number is not grossly insufficient.

The Reynolds stresses and their dependence on  $\text{Re}$  are illustrated in Fig. 4. (Henceforth, only Code C results will be considered.) We have already mentioned the similarity of the FPG-wall scaled stresses (Fig. 4a) to those observed in the plane channel; the significant variation with Reynolds number of all three normal stresses measured in units of  $u_\tau$  versus  $y^+$  has been noted in many studies (without, however, any certainty

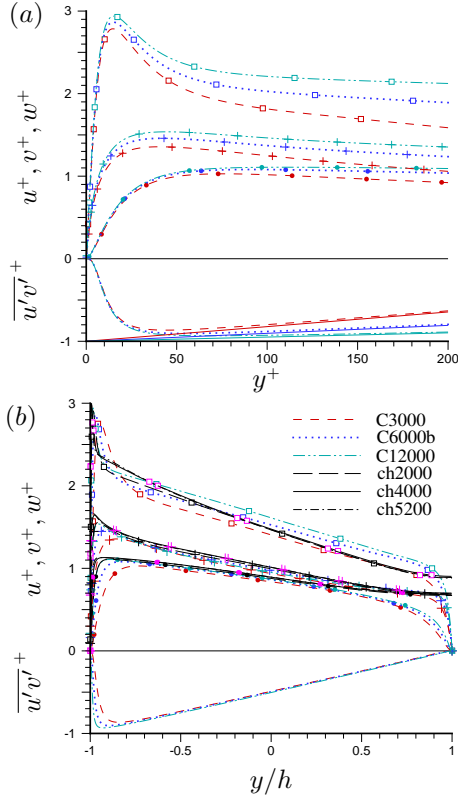


Figure 4: FPG-wall scaling of Reynolds-shear-stress and turbulence-intensity profiles:  $\square$ ,  $u^+ = \sqrt{u'u'}/u_\tau$ ;  $\bullet$ ,  $v^+ = \sqrt{v'v'}/u_\tau$ ;  $+$ ,  $w^+ = \sqrt{w'w'}/u_\tau$ ; no symbol,  $\overline{u'v'}^+ = \overline{u'v'}/u_\tau^2$ . Slope of solid lines in (a) corresponds to  $-p^+ = -[d(P/\rho)/dx][\nu/u_\tau^3]$ . Cases ch2000, ch4000 and ch5200 in (b) are from plane-channel ( $U_w \equiv 0$ ) DNS of, respectively, Hoyas & Jiménez 2006 ( $R_\tau = 2003$ ), Bernardini *et al.* 2014 ( $R_\tau = 4079$ ) and Lee & Moser 2015 ( $R_\tau = 5186$ ), where for illustration purposes the wall-to-centerline half-domain from that flow has been mapped to the full bottom-to-top-wall domain here.

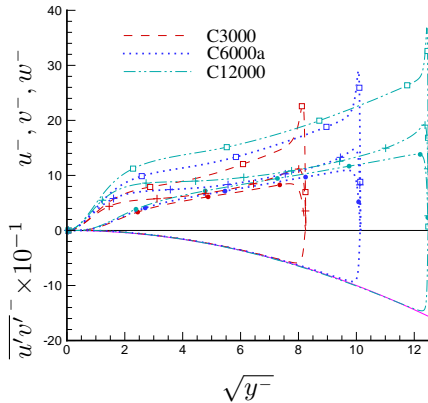


Figure 5: APG-wall scaling of Reynolds-shear-stress and turbulence-intensity profiles with respect to  $y^- = (y - h)u_p/\nu$ :  $\square$ ,  $u^- = \sqrt{u'u'}/u_p$ ;  $\bullet$ ,  $v^- = \sqrt{v'v'}/u_p$ ;  $+$ ,  $w^- = \sqrt{w'w'}/u_p$ ; no symbol,  $\overline{u'v'}^- = \overline{u'v'}/u_p^2$ . Solid line traces theoretical variation,  $-\overline{u'v'}^- = y^-$

on whether this is a ‘low-Reynolds-number effect’ that will ultimately saturate). The collapse and linear behavior in the core-layer variable  $y/h$  of the  $-\overline{u'v'}$  shear stresses across the core is required in this scaling (Fig.4b). The wall-normal  $v^+$  and spanwise  $w^+$  components also tend to collapse in the core region, as they do in pure Poiseuille flow (when their ‘folded’ wall-to-centerline half domains are expanded to fill the full bottom-to-top wall domain of the present CP0 flow, as is done in Fig. 4b for the  $u_\tau h/\nu = 2000, 4000$  and  $5200$  DNS of Hoyas & Jiménez (2006), Bernardini *et al.* (2014) and Lee & Moser (2015), respectively.) The behavior of the streamwise component  $\sqrt{\overline{u'u'}}$ , on the other hand, differs from that of the  $U_w = 0$  case, for which only in the inner layer and bottom of the outer layer does it become an increasingly large fraction of  $u_\tau$  as Reynolds number increases. Here the profiles remain linear across the bulk of the flow and the step with Re appears almost uniform in space, and identical for the two Reynolds-number doublings, so that there is little indication that the rise will saturate rapidly at even higher Re.

The Reynolds stresses in the zero-stress-wall scaling are presented in Fig.5. The  $-\overline{u'v'}$  component agrees well with the theoretical profile,  $-\overline{u'v'}^- = y^-$ , for each of the three Reynolds numbers, as required by the momentum balance; the viscous stress is not visible in these coordinates except near the opposite wall. This agreement also suggests the success of the pressure-gradient-and-wall-velocity combinations used here to establish the CP0 conditions. As is the case for the FPG-side fluctuations in the  $u_\tau$  scaling, the normal-stress components in the  $u_p$  scaling fail to exhibit Reynolds-number independence, with the deviation for the streamwise component being especially pronounced. Thus, the turbulence as a whole definitely does not scale with only  $u_p$  and  $y^-$  even if the velocity and shear stress do.

The instantaneous streamwise velocity contours in a  $y-z$  plane shown in Fig. 6 suggest the turbulence associated with the FPG wall affects the flow all the way to the APG side. Eruptions from the intense FPG region reach close to the quiescent APG layer. This does not appear to defeat the Stratford argument. This figure also suggests that the domain size is quite adequate, since (unlike in pure Couette flow) there is no evidence of very large flow structures which would be confined by the periodic conditions.

## 4 Summary and Future Work

Our joint study of the Couette-Poiseuille flow with zero skin friction on one wall by Direct Numerical Simulation reached its objectives quite well. Away from the zero-skin-friction wall the mean velocity is dominated by the friction velocity  $u_\tau$  and the channel half-height  $h$ , as it is in simple Poiseuille flow. The results are consistent with the formation of a logarithmic



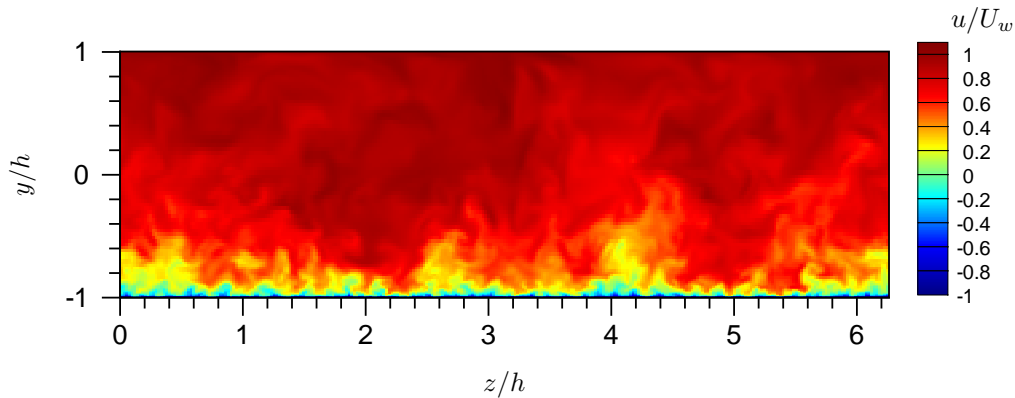


Figure 6: Instantaneous contours of streamwise velocity  $u$  in cross-stream-vertical plane from CP0 DNS presented in CS15 ( $Re = 10000$ ).

mic layer at even higher Reynolds number, but suggest an unexpectedly low Karman constant, in the vicinity of 0.36. This thorny issue is very present in DNS of Poiseuille flow by other groups, in which a clear determination of the Karman constant has been elusive. The streamwise Reynolds stress is again not universal with any normalization we attempted, but we do not believe the two issues are related.

In the future, higher Reynolds numbers may refine the estimates of the Stratford constants. Some variation of the periodic domain size is in order, but is not expected to alter the conclusions. An experiment on the CP0 flow would be of great interest, provided accurate measurements are possible close enough to a sliding belt, and a large enough domain eliminates end effects in both directions. The CP0 flow also becomes a candidate to be a standard calibration case for turbulence models. We have determined that models of the classical type will naturally satisfy Stratford scaling and produce square-root layers, but for instance the Spalart-Allmaras model does not give very accurate values for the  $B$  and  $C$  constants.

Looking beyond the ideal CP0 situation, it will be of great interest to explore other flows with zero skin friction. For instance, a separating boundary layer may or may not sustain zero skin friction over a large enough region for the scaling to establish itself. The mean wall-normal velocity  $V$ , or the strain  $\partial V/\partial y$ , may also conflict with the pressure gradient as a dominating influence. We have DNS in which the skin friction *crosses* zero, but not of Stratford's 'continuously separating' flow, which will be quite challenging because the boundary-layer thickness increases so rapidly.

## Acknowledgments

This project was sponsored in part by the Revolutionary Computational Aerosciences project under NASA's Fundamental Aerodynamics program. Computations were performed on resources provided by the NASA Advanced Supercomputing (NAS) Division, while the results of the Sapienza unit have been

achieved using the PRACE Research Infrastructure resource FERMI based at CINECA, Casalecchio di Reno, Italy.

## References

- Bernardini, M., Pirozzoli, S. and Orlandi, P. (2014), Velocity statistics in turbulent channel flow up to  $Re_\tau = 4000$ , *J. Fluid Mech.*, Vol. 742, pp. 171-191.
- Coleman, G.N. and Spalart, P.R. (2015), Direct numerical simulation of turbulent Couette-Poiseuille flow with zero skin friction, *Proceedings of 15th European Turbulence Conference*, 25-28 August, 2015, Delft, The Netherlands (referred to herein as CS15).
- Hoyas, S. and Jiménez, J. (2006), Scaling of the velocity fluctuations in turbulent channels up to  $Re_\tau = 2003$ , *Phys. Fluids*, Vol. 18, 011702.
- Johnstone, R., Coleman, G.N. and Spalart, P.R. (2010), The resilience of the logarithmic law to pressure gradients: evidence from direct numerical simulation, *J. Fluid Mech.*, Vol. 643, pp. 163-175.
- Lee, M. and Moser, R.D. (2015), Direct numerical simulation of turbulent channel flow up to  $Re_\tau \approx 5200$ , *J. Fluid Mech.*, Vol. 774, pp. 395-415.
- Luchini, P. and Quadrio, M. (2006), A low-cost parallel implementation of direct numerical simulation of wall turbulence, *J. Comp. Phys.*, Vol. 211 (2), pp. 551-571.
- Orlandi, P. (2000), *Fluid Flow Phenomena: A Numerical Toolkit*, Kluwer.
- Pirozzoli, S., Bernardini, M. and Orlandi, P. (2011), Large-scale motions and inner/outer layer interactions in turbulent Couette-Poiseuille flows, *J. Fluid Mech.*, Vol. 680, pp. 534-563 (referred to herein as PBO11).
- Schlichting, H. and Gersten, K. (2000), *Boundary Layer Theory* (8th edition), Springer.
- Spalart, P.R., Coleman, G.N. and Johnstone, R. (2009), Retraction: 'Direct numerical simulation of the Edman layer: A step in Reynolds number, and cautious support for a log law with a shifted origin', *Phys. Fluids*, Vol. 21, 109901.
- Stratford, B.S. (1959), The prediction of separation of the turbulent boundary layer, *J. Fluid Mech.*, Vol. 5, pp. 1-16.
- Townsend, A.A. (1976), *The Structure of Turbulent Shear Flow* (2nd edition), Cambridge.